



Title	Numerical Model of Gas Metal Arc with Metal Vapor for Heat Source in Welding
Author(s)	Tsujimura, Yoshihiro; Tashiro, Shinichi; Tanaka, Manabu
Citation	Transactions of JWRI. 2011, 40(1), p. 25-29
Version Type	VoR
URL	https://doi.org/10.18910/6896
rights	
Note	

The University of Osaka Institutional Knowledge Archive : OUKA

<https://ir.library.osaka-u.ac.jp/>

The University of Osaka

Numerical Model of Gas Metal Arc with Metal Vapor for Heat Source in Welding[†]

TSUJIMURA Yoshihiro*, TASHIRO Shinichi** and TANAKA Manabu***

Abstract

In gas metal arc (GMA) welding, an arc discharge is applied for melting and joining metals. An electric arc is established between a base metal cathode and a consumable wire anode. By the high heat flux from the arc plasma, a droplet forms at the tip of wire and a weld pool forms at the base metal. Arc plasma is composed of large amounts of metal vapor from the droplet and the weld pool. From past studies, it is known that a mixture of metal vapor affects the properties of the arc plasma, such as electrical conductivity and radiative emission coefficient. Numerical models need many assumptions and time for complicated calculations. Therefore, to reduce assumptions and calculation time, a simplified model of the GMA welding arcs ignoring metal transfer is built. In the present model, special account is taken of the amounts of metal vapor, enthalpy of droplet and wire melting rate. These are calculated simultaneously. And then, the present model assumes a steady state, and that arc length is constant. Therefore, the wire feed rate is equal to the calculated wire melting rate. And then, the wire feed rate and the wire melting rate are balanced to keep arc length constant. We study the effects of metal vapor on the heat source properties of GMA welding arcs by using this model. The calculated mole fraction distribution is in agreement with the observed optical image separating bright regions at the arc center, dominated by the metal vapor, and dark regions at the outer arc. The highest temperatures occur at the edge of the arc core. Higher welding currents lead to faster melting and feed rates of consumable wire because of larger heat inputs, such as thermal conduction from the arc plasma and ohmic heating at the wire. For balance of larger heat inputs and faster feed rates of the wire, temperatures of the tip of wire, namely droplet, are kept constant though higher welding currents. This result is experimentally known, however this model enable it to be understood as a physical phenomenon.

KEY WORDS: (GMA welding), (Metal vapor), (Simulation)

1. Introduction

In gas metal arc (GMA) welding, an arc discharge is applied for melting and joining metals. An electric arc is established between a base metal cathode and a consumable wire anode. By the high heat flux from arc plasma, a droplet forms at the tip of the wire and a weld pool forms at the base metal. Arc plasma is composed of large amounts of metal vapor from the molten wire, the droplet and the weld pool. From past studies, it is known that mixture of metal vapor affects the properties of the arc plasma, such as electrical conductivity and radiative emission coefficient [1, 2].

Because of many forces and interactions between arc and electrodes, understanding of GMA welding is difficult. Studies about GMA welding model have been presented [3-5]. Shnick [3] and Haidar [4] showed that the temperature at arc center became low due to evaporation of metal vapor. Fan [5] succeeded in the

simulation of GMA welding with metal transfer. However, interactions between electrodes and arc plasma are not taken into account, although the amount of metal vapor from the wire is constant though wire temperature changes in these models. In the present paper, to research effects of metal vapor on GMA welding in detail, a model of GMA welding arcs without metal transfer is proposed.

The mixture of metal vapor affects arc plasma in gas tungsten arc (GTA) welding in which metal vapor evaporates only from the weld pool [2]. We can guess easily that a mixture of metal vapor affects arc plasma much more in GMA welding because metal vapor evaporates from the molten wire, the droplet and the weld pool. Heat input to the base metal depends on the state of arc plasma, and then welding results, like weld penetration, depends on the heat input to the base metal. Therefore, the heat input to the base metal is very

† Received on June 10, 2011

* Graduate School Student

** Assistant Professor

*** Professor

Transactions of JWRI is published by Joining and Welding Research Institute, Osaka University, Ibaraki, Osaka 567-0047, Japan

important as a heat source property. The present model can calculate this heat source property. We study the effects of metal vapor on the heat source property of GMA welding arcs by using this model.

2. Simulation model

In the present model, GMA welding without metal transfer is assumed. A wire, arc plasma and a base metal are described relative to cylindrical coordinates, assuming rotational symmetry around the arc axis. The calculation domain is shown in **Figure 1**. The diameter of the wire anode is 1.2mm. The base metal is stainless steel. Argon shielding gas is introduced from the outside of the wire on the upper boundary at the flow rate of 10L/min. Welding current flows from the wire to the base metal. Namely, the wire is anode and the base metal is cathode, and this model assumes reverse polarity.

The governing equations used in the models are shown as follows:

The mass continuity equation is,

$$\frac{1}{r} \frac{\partial}{\partial r} (r \rho v_r) + \frac{\partial}{\partial z} (\rho v_z) = S \quad (1)$$

The radial momentum conservation equation is,

$$\begin{aligned} \frac{1}{r} \frac{\partial}{\partial r} (r \rho v_r^2) + \frac{\partial}{\partial z} (\rho v_z v_r) = \\ - \frac{\partial p}{\partial r} - j_z B_\theta + \frac{1}{r} \frac{\partial}{\partial r} \left(2r\eta \frac{\partial v_r}{\partial r} \right) + \frac{\partial}{\partial z} \left(\eta \frac{\partial v_r}{\partial z} + \eta \frac{\partial v_z}{\partial r} \right) - 2\eta \frac{v_r}{r^2} \end{aligned} \quad (2)$$

The axial momentum conservation equation is,

$$\begin{aligned} \frac{1}{r} \frac{\partial}{\partial r} (r \rho v_r v_z) + \frac{\partial}{\partial z} (\rho v_z^2) = \\ - \frac{\partial p}{\partial z} - j_r B_\theta + \frac{\partial}{\partial z} \left(2\eta \frac{\partial v_z}{\partial z} \right) + \frac{1}{r} \frac{\partial}{\partial r} \left(r\eta \frac{\partial v_r}{\partial z} + r\eta \frac{\partial v_z}{\partial r} \right) + \rho g \end{aligned} \quad (3)$$

The energy conservation equation is,

$$\begin{aligned} \frac{1}{r} \frac{\partial}{\partial r} (r \rho v_r h) + \frac{\partial}{\partial z} (\rho v_z h) = \\ \frac{1}{r} \frac{\partial}{\partial r} \left(\frac{r\kappa}{c_p} \frac{\partial h}{\partial r} \right) + \frac{\partial}{\partial z} \left(\frac{\kappa}{c_p} \frac{\partial h}{\partial z} \right) + j_r E_r + j_z E_z - U \end{aligned} \quad (4)$$

The current continuity equation is,

$$\frac{1}{r} \frac{\partial}{\partial r} (r j_r) + \frac{\partial}{\partial z} (j_z) = 0 \quad (5)$$

$$j_r = -\sigma E_r, j_z = -\sigma E_z \quad (6)$$

where, t is time, h is enthalpy, p is pressure, v_r and v_z are radial and axial velocities, S is vaporization rate [6], j_r and j_z are the radial and axial components of the current density, g is acceleration due to gravity, c_p is specific heat, κ is thermal conductivity, ρ is density, η is viscosity, U is radiative emission coefficient, and σ is electrical conductivity. E_r and E_z are the radial and axial components of the electric field defined by:

$$E_r = -\frac{\partial V}{\partial r}, \quad E_z = -\frac{\partial V}{\partial z} \quad (7)$$

where, V is electric potential.

The azimuthal magnetic field, B_θ induced by arc current is evaluated by Maxwell's equation:

$$\frac{1}{r} \frac{\partial}{\partial r} (r B_\theta) = \mu_0 j_z \quad (8)$$

where, μ_0 is the permeability of free space.

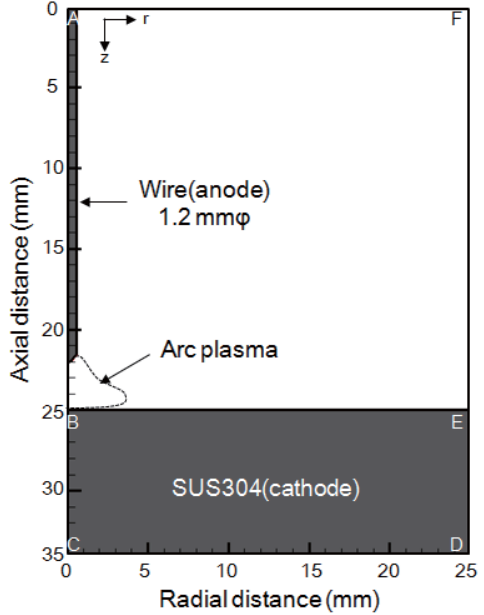


Fig. 1 Schematic illustration of simulation domain.

It is necessary to consider the effects of energy transfer at the electrode surfaces. The additional energy fluxes at the cathode and anode are described as:

$$\text{Cathode: } F_K = -\varepsilon\alpha T^4 - |j_e|\phi_K + |j_i|V_i + \rho V_M h_p \quad (9)$$

$$\text{Anode: } F_A = -\varepsilon\alpha T^4 - |j|\phi_A \quad (10)$$

where, ε is surface emissivity, α is the Stefan-Boltzmann constant, ϕ_K is the work function of the cathode, V_i is the ionization potential of the plasma gas, j_e is the electron current density, j_i is the ion current density, ϕ_A is the work function of the anode and T is the temperature. For the cathode surface, F_K needs to be included in Equation (4) to take into account the thermionic cooling by emission of electrons, radiative cooling and ion heating. Similarly, for the anode surface, F_A is required in Equation (4) to take into account radiative cooling and thermionic heating. Furthermore, for the cathode surface, the electron current and the ion current are considered separately and defined based on the Richardson-Dushman equation of thermionic emission as follows:

$$j_r = AT^2 \exp\left(-\frac{e\phi_K}{k_B T}\right) \quad (11)$$

where, k_B is the Boltzmann's constant and A is the Richardson's constant, which depends on the cathode material. The ion current density, j_i is then assumed to be $j_i = j - j_r$, where the total current density, j is $|j| = |j_e| + |j_i|$.

A species conservation equation expressed by Eq. (12) is applied to take a metal vapor behavior into account [2]. To simplify the model and facilitate calculation, only iron vapor is considered in present model. In the present model, plasma properties are dependent on the temperature and the mole fraction of iron vapor.

$$\frac{1}{r} \frac{\partial}{\partial r} (r \rho v_r C_1) + \frac{\partial}{\partial z} (\rho v_z C_1) = \frac{1}{r} \frac{\partial}{\partial r} \left(r \rho D \frac{\partial C_1}{\partial r} \right) + \frac{\partial}{\partial z} \left(\rho D \frac{\partial C_1}{\partial z} \right) + S \quad (12)$$

where, C_1 is the mass fraction concentration of iron vapor and D is the two-dimensional diffusion coefficient which is expressed by the viscosity approximation equation:

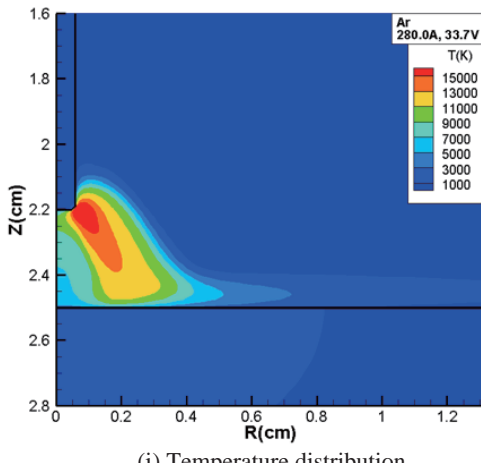
$$D = \frac{2\sqrt{2}(1/M_1 + 1/M_2)^{0.5}}{\left\{ \left(\rho_1^2 / \beta_1^2 \eta_1^2 M_1 \right)^{0.25} + \left(\rho_2^2 / \beta_2^2 \eta_2^2 M_2 \right)^{0.25} \right\}^2} \quad (13)$$

where, M_1 and M_2 are the molecular weights of iron and the shielding gas, respectively. ρ_1 , ρ_2 , η_1 and η_2 are the density and viscosity of iron and argon gas, respectively. β_1 and β_2 are dimensionless constants, and theoretically range from 1.2 to 1.543 for various kinds of gas. $\beta_1 = \beta_2 = 1.385$ is assumed based on the mean value of the experimental data [7]. The amount of metal vapor is referred from experimental results of DebRoy [6]. And then, the amount of metal vapor depends on the surface temperature of electrodes. Plasma properties at intermediate concentrations of iron vapor are calculated using a linear approximation based on the properties at 0mol%, 1mol%, 10mol%, 20mol%, 30mol% and 100mol% [2]. The properties were calculated assuming the arc plasma to be in local thermodynamic equilibrium (LTE), and using the Chapman-Enskog approximation [1].

Approximations, governing equations and boundary conditions are given in detail in our previous papers [2]. The governing and auxiliary equations are solved iteratively by the SIMPLEC numerical procedure.

In the present model, special accounts are taken of the amount of metal vapor, enthalpy of the droplet and a wire melting rate. These are calculated simultaneously. The present model assumes a steady state, and that arc length is constant. Therefore, the wire feed rate is equal to the calculated wire melting rate. And, the wire feed rate and the wire melting rate are balanced to keep arc length constant. The wire feed rate affects the temperature distribution of the wire. Wire melting rate is expressed by equation [8, 9]:

$$V_M = \frac{1}{\rho h_p} (\phi \cdot j + \gamma_0 L \cdot j^2) \quad (14)$$



(i) Temperature distribution

where V_M is wire melting rate, ρ is the density, h_p is enthalpy of droplet, ϕ is equivalent voltage of melting of arc welding, j is current density, γ_0 is electrical conductivity at contact tip and L is wire length. Wire melting rate is determined by Joule heat of wire and thermal conduction from arc plasma.

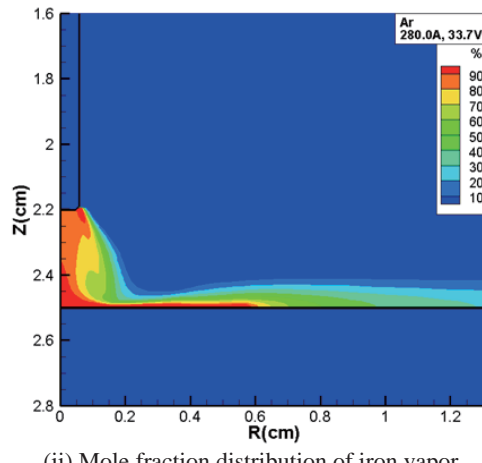
Enthalpy of droplet is needed to calculate wire melting rate and heat transfer of droplet towards the base metal. Firstly, the droplet region assumes the area where temperature is over the melting point at the tip of wire. The enthalpy of the droplet is calculated from the average temperature of the droplet region. And then, wire melting rate is given by equation (14). $\rho h_p V_M$ is added to the base metal as heat transfer of droplet, therefore energy balance is taken account.

Present model takes account of welding speed (60cm/min). However, because the present model assumes cylindrical coordinates, welding speed can't be built into the model directly. Therefore, the energy cooling effect with torch movement is removed in each cell, and then quasi welding speed is taken into account. Treatment of the cathode is considered in the present model. The cathode in the arc discharge is classified hot cathode and cold cathode according to mechanisms of electron emission. Hot cathode emits electron by thermionic emission, and cold cathode emits by field emission. Field emission needs a strong electric field at the cathode surface. Electric field is not so strong that electrons emit enough in GMA welding. Therefore, the hot cathode is assumed, and a work function of the cathode is set to be 3.85eV as iron oxide. This model is taken into account of cathode fall. In the present model, cathode fall is total of space charge [10] and equivalent voltage for ionization.

We make an inconsistent model with little assumptions by iterative calculation with feedback output data.

3. Calculation results

Figure 2 shows simulation results of temperature



(ii) Mole fraction distribution of iron vapor

Fig. 2 Simulation results of GMA welding with welding current of 280A.

Numerical Model of Gas Metal Arc with Metal Vapor for Heat Source in Welding

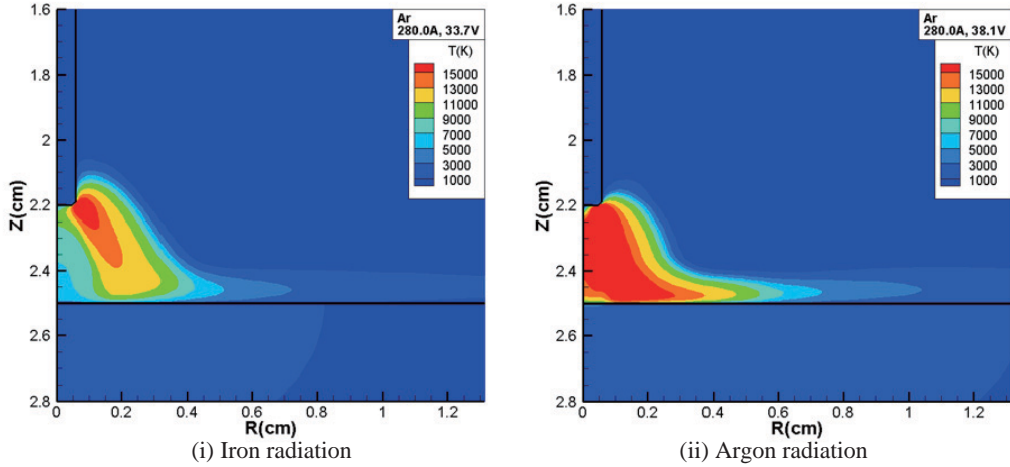


Fig. 3 Simulation results of temperature field in GMA welding that radiation of metal vapor is set to be iron and argon property.

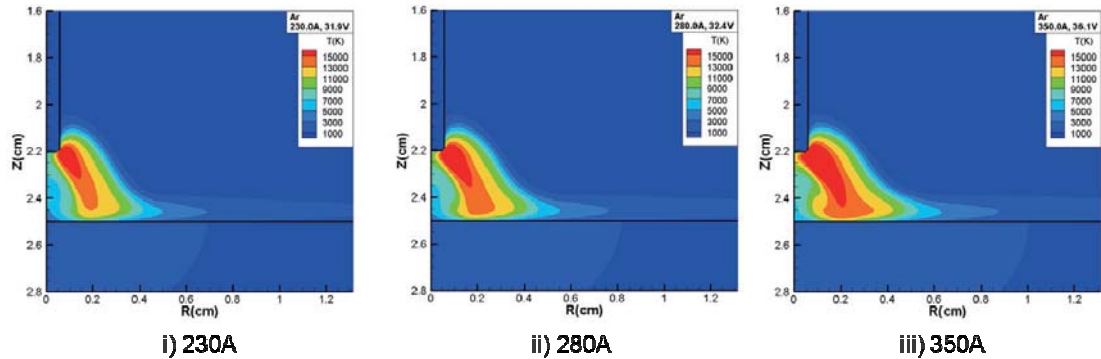


Fig. 4 Simulation results of temperature field in GMA welding with welding current of 230, 280 and 350A

Table 1 Simulation results of wire melting rate and droplet temperature in GMA welding with welding current of 230, 280 and 350A.

Welding current [A]	Wire melting rate [m/min]	Droplet temperature [K]
230	8.2	2481
280	10.0	2535
350	13.7	2593

distribution and mole fraction distribution of iron vapor in GMA welding with a welding current of 280A. The calculation of mole fraction distribution is in agreement with the calculation results of Schnick [3]. The highest temperatures occur at the edge of the arc core. Droplet temperature becomes 2535K, maximum surface temperature of weld pool becomes 2243K. The temperature of arc plasma becomes highest near the wire edge, and the temperature becomes about 7000K at the arc center. Arc voltage becomes 32.4V, electric power becomes 9072W, and heat input to base metal becomes 6116W, therefore heat efficiency is 67.4%. Almost all of the energy loss is radiative. Information on voltage and heat efficiency is very important for welding control. The

amount of iron vapor evaporated from wire become 0.0038g/s. Wire melting rate and feed rate become 10.0m/min.

Figure 3 shows simulation results of temperature field in GMA welding with argon radiation instead of iron radiation. This simulation result shows high temperature at the arc center in GMA welding with argon radiation. Because iron vapor has strong radiation, energy loss of radiation increases with increase of concentration of iron vapor. In GMA welding process, the temperature of the arc plasma is low because energy loss of radiation is large at the region where iron vapor dominates.

Figure 4 shows simulation results of temperature field in GMA welding with welding currents of 230A,

280A and 350A. The temperature of the arc plasma depends on welding current. Table 1 shows simulation results of wire melting rate and droplet temperature. Higher welding currents lead to faster melting and feed rates of consumable wire because of larger heat inputs, such as thermal conduction from the arc plasma and ohmic heating at the wire. For balance of larger heat inputs and faster feed rates of the wire, temperatures of droplet are kept constant though higher welding currents. This result is experimentally known, however this model enable it to be understood as a physical phenomenon.

4. Conclusions

We build a GMA welding model ignoring metal transfer, and we study effects of metal vapor on heat source properties of GMA welding arcs. The conclusions of this work are summarized as follows.

- (1) In GMA welding, the highest temperatures occur at the edge of the arc core.
- (2) Iron vapor from the tip of the wire dominate at the arc center.
- (3) Because energy loss of radiation is large at region where iron vapor dominate, temperature of arc plasma becomes low.

- (4) For balance of larger heat inputs and faster feed rates of the wire, droplet temperature is kept constant though higher welding currents.

References

- [1] Murphy AB: *J. Phys. D: Appl. Phys.*, 42(2009), p.194006.
- [2] Yamamoto K, et al: *Surface & Coating Technology*, 202(2008), pp.5302-5305.
- [3] Schnick M, et al; *J. Phys. D: Appl. Phys.*, 43(2010), p.022001.
- [4] Haidar J: *J. Phys. D: Appl. Phys.*, 43(2010), p.165204.
- [5] Fan HG and Kovacevic R: *J. Phys. D: Appl. Phys.*, 37(2004), pp.2531-2544.
- [6] DebRoy T, et al: *J. Phys. D: Appl. Phys.*, 70(1991), pp.1313-1319.
- [7] Wilke CR: *J. Chem. Phys.*, 18(1950), pp.517-519.
- [8] Ushio M and Mao W: *Quarterly J. Japan Welding Soc.*, 14(1996), pp.99-107.
- [9] Nakamura T and Hiraoka K: *Quarterly J. Japan Welding Soc.*, 20(2002), pp.53-62.
- [10] Ushio M, Fan D and Tanaka M: *J. Phys. D: Appl. Phys.*, 27(1994), pp.561-566.